

Original Article



Differences in Leukocyte Transcriptomes of Morbidly Obese Patients With High Output Heart Failure: A Pilot Study

Samantha A. Cintron , PhD, RN¹, Janet Pierce , PhD, APRN, CCRN, FAAN¹, Mihaela E. Sardi , PhD², Diane Mahoney , PhD, DNP, FNP-BC, WHNP-BC¹, Jill Peltzer , PhD, APRN-CNS¹, Bhanu Gupta , MD, MSc³, and Qiuhua Shen , PhD, APRN¹

¹School of Nursing, University of Kansas Medical Center, Kansas City, KS, USA

²Department of Biostatistics & Data Science, University of Kansas Medical Center, Kansas City, KS, USA

³Department of Cardiovascular Medicine, University of Kansas Medical Center, Kansas City, KS, USA



Received: May 17, 2023

Revised: Aug 2, 2023

Accepted: Aug 17, 2023

Published online: Sep 5, 2023

Correspondence to

Samantha A. Cintron, PhD, RN

School of Nursing, University of Kansas Medical Center, Mail Stop 4043, 3901 Rainbow Blvd, Kansas City, KS 66160, USA.

Email: sjohnson18@kumc.edu

Copyright © 2023. Korean Society of Heart Failure

This is an Open Access article distributed under the terms of the Creative Commons Attribution Non-Commercial License (<https://creativecommons.org/licenses/by-nc/4.0>) which permits unrestricted noncommercial use, distribution, and reproduction in any medium, provided the original work is properly cited.

ABSTRACT

Background and Objectives: Heart failure is characterized by alterations of gene expression that provide insight into the underlying pathophysiologic mechanisms. However, obesity-related high output heart failure (HOHF) is a specific phenotype of heart failure that has not been studied using gene expression. Our aim in this study was to examine the variances in leukocyte transcriptomes of morbidly obese patients with HOHF.

Methods: In this cross-sectional study, we applied stranded total RNA-sequencing to six patients with morbid obesity and HOHF and 6 patients with morbid obesity and non-HOHF. Differential gene expression was calculated, and Ingenuity Pathway Analysis software was used to interpret the canonical pathways, functional changes, upstream regulators, and networks in these patients.

Results: We found in patients with HOHF that there were 116 differentially expressed genes with upregulation of 114 genes and downregulation of 2 genes. The differentially expressed genes were involved with cell proliferation, mitochondrial function, erythropoiesis, erythrocyte stability, and apoptosis. The top upregulated canonical pathways associated with differentially expressed genes were autophagy, adenosine monophosphate-activated protein kinase signaling, and senescence pathways. We identified GATA binding protein 1 as an upstream regulator and nuclear factor kappa-light-chain-enhancer of activated B cells associated network.

Conclusions: We are the first to report the differential gene expression in patients with obesity-related HOHF and reveal the various pathophysiologic mechanisms underlying the disease. Further research is needed to determine the role of cellular function and maintenance, inflammation, and iron homeostasis in obesity-related HOHF.

Keywords: Obesity; Heart failure; Genomics; Cardiac output, high

INTRODUCTION

Heart failure (HF) is a complex pathophysiologic state that presents with different phenotypes.¹ While HF is usually associated with a cardiac structural or functional abnormality that results in a low cardiac output (CO; <5 L/min), a less common phenotype of HF is high output heart failure (HOHF).^{1,2} In HOHF, patients experience symptoms of HF because the metabolic demands of the body are not being met despite maintaining high CO (≥ 8 L/min) or cardiac index (CI; > 3.9 L/min/m²). Obesity is a common cause of HOHF and patients with obesity-related HOHF are often undiagnosed or misclassified as heart failure with preserved ejection fraction (HFpEF) based on left ventricular ejection fraction (LVEF) $> 50\%$ because the CO and CI are not always available to differentiate HOHF from HFpEF. In clinical practice, LVEF is a universally known variable index used to classify patients with HF that is easily estimated by imaging techniques, mainly echocardiography. Invasive hemodynamic assessment is required to diagnose HOHF which is not routinely performed in the HF patient population.^{1,2}

Obesity is a significant underlying disease that accounts for HOHF. Morbid obesity is used to describe individuals with a body mass index (BMI) of 40 kg/m² or greater or a BMI of 35 kg/m² or greater with obesity-related health conditions.³ Obesity can be classified as a primary disease because the adipocyte hypertrophy alters the secretion of hormones that can lead to the dysregulation of metabolic pathways and results in a pro-inflammatory status. The hormones produced by adipocytes are called adipokines and dysregulation of adipokines contributes to development of cardiovascular disease.⁴

Circulating leukocytes have been proposed as a potential source of HF biomarkers since they can be obtained in a minimally invasive manner.^{5,6} In addition, leukocytes contain various cell organelles and RNA is synthesized in the leukocyte.⁶ Sensitive to the metabolic and biochemical environment, circulating leukocytes interact with organs and thus, gene expression changes in leukocytes could be reflective of a diseased organ.^{6,7} Of the 12,440 genes expressed in the myocardium, 84.2% of those genes are also expressed in the blood.⁷ Current knowledge of the role of leukocytes in systemic inflammation associated with comorbidities, inflammation associated with HF initiation and progression, and left ventricular remodeling supports the concept that leukocyte transcriptome alterations help inform about heart function status and disease progression.⁶ High-throughput RNA sequencing (RNA-seq) provides the instrumentation for investigators to discover the differential gene expression and determine the molecular dysregulation that causes obesity-relat-

ed HOHF. Therefore, we investigated the differences in leukocyte transcriptomes of morbidly obese patients with HOHF and those with non-HOHF using RNA-seq. We then utilized Ingenuity Pathway Analysis (IPA) software to identify the canonical pathways, functional changes, upstream regulators, and mechanistic and causal networks associated with the significantly different leukocyte transcriptomes.

METHODS

For detailed methods, see expanded methods in the **Supplementary Data 1**.

Study population

The study was approved by the Institutional Review Board at the University of Kansas Medical Center (KUMC). This study was performed in line with the principles of the Declaration of Helsinki. Written informed consent was obtained from all participants.

A total of 12 patients with morbid obesity and HF were recruited in the study: six patients with HOHF (CO ≥ 8 L/min or CI > 3.9 L/min/m²) and six patients with non-HOHF (CO < 8 L/min and CI ≤ 3.9 L/min/m²). Patients over the age of 18 were eligible for inclusion in the study. They had a BMI ≥ 30 kg/m², diagnosis or signs and symptoms of HF, left ventricular ejection fraction $\geq 45\%$, scheduled or recent (within the last 12 months) right heart catheterization, and were English speaking. Exclusion criteria included severe systemic illness with life expectancy less than 2 years; an alternative identifying cause of HOHF other than obesity (e.g., pregnancy, severe anemia, thyrotoxicosis, liver failure, chronic lung disease, and arteriovenous malformations); atrial fibrillation (heart rate > 90 beats per minute); myocardial infarction, coronary artery bypass graft surgery, or cerebrovascular accident in the last 90 days; percutaneous coronary intervention in the past 30 days; heart transplant; left ventricular assist device; orthostatic hypotension; constrictive pericarditis; and cardiomyopathies.

Patients were screened for eligibility prior to a scheduled appointment. After obtaining written informed consent, a blood sample (8 mL) was collected in a heparinized green-top tube from the patients. Additionally, basic demographic data (age, birth sex, race, and ethnicity) and clinical data were collected from the electronic medical record (EMR). Measures of CO and CI using the Fick principle were recorded during a right heart catheterization for comparison between the groups and to verify high output status. A one-time incentive of \$25 was provided to the patient in the form of ClinCard after completing all study requirements.

RNA-extraction, library preparation, and sequencing

The blood sample was immediately sent to the KUMC Biomarker Core for isolation of leukocytes the same day as the blood draw and stored at -80°C until all samples were collected. Invitrogen's TRIzol Reagent (Thermo Fisher Scientific, Waltham, MA, USA) was used to isolate total RNA per manufacturer's protocol. Immediately after isolation, all RNA samples were transported on dry ice to the KUMC Genomics Core for RNA-sequencing. Stranded total RNA-seq was performed.

Statistical analysis and bioinformatics

Descriptive statistics for all demographic and clinical variables were calculated using IBM SPSS Statistics (version 27.0; IBM Corp., Armonk, NY, USA). χ^2 tests and Mann Whitney U test were used to identify group differences in demographic and clinical characteristics. Sequence data generated by the Illumina NovaSeq 6000 was processed by Real Time Analysis software and deposited on the iCompute Server. Sequence data were converted from the .bcl file format to fastQ files and de-multiplexed into individual sequences for downstream analysis. The RNA-seq data were checked for quality using the FastQC method. All samples passed the quality check and were aligned and quantified to human genome using bowtie2 and RSEM libraries. Transcript quantification data were analyzed to find reads per kilobase per million mapped reads values and a gene count matrix was developed.

The gene count matrix was analyzed using empirical analysis of digital gene expression data in R (edgeR).⁸⁾ The data were filtered to remove genes which did not occur frequently enough for analysis. Next the data were normalized by finding a set of scaling factors that minimizes the log-fold changes between the samples for most genes. Common and tagwise dispersions were estimated using the quantile-adjusted conditional maximum likelihood (qCML) method. Next, the exact test in edgeR was used to determine differential expression. A Benjamini-Hochberg adjusted p value of ≤ 0.05 and a $\log_2(\text{fold-change})$ of ± 1 were used to determine if genes were differentially expressed. Lastly, differentially expressed genes (DEGs) were visualized in a heatmap.⁹⁾

There were four major IPA core analyses that assisted with the analysis, integration, and understanding of gene expression data: 1) Canonical Pathway Analysis, 2) Disease and Function Analysis, 3) Upstream Regulator Analysis, and 4) Networks Analysis.¹⁰⁾ Fisher's exact test was used in all IPA core analyses and determined the p value of overlap. The z-score was used to determine activation or inhibition of a molecule or pathway and a z-score of 0 indicated that the two groups had similar levels of the molecule or pathway.

RESULTS

Characteristics of the sample

Demographic and clinical data of patients who participated in the study are displayed in **Table 1**. The median age was 61 years old (range, 39–79) for subjects in the HOHF group and 73.5 years old (range, 58–86) for those with non-HOHF. The HOHF group had a higher percentage of males (66%) than the non-HOHF group (50%). The subjects in the non-HOHF group identified primarily as White (n=5, 83.33%) while 50% of the HOHF group (n=3) selected "Other" for race and identified as Hispanic or Latino for ethnicity. All the subjects in the non-HOHF group identified as not Hispanic or Latino. The BMIs of the HOHF group and non-HOHF group were 39.97 kg/m^2 (range, 30.10–80.18) and 38.19 kg/m^2 (range, 35.15–43.58), respectively. As expected, subjects in the HOHF group had a significantly greater CO (9.45 L/min) and CI (4.65 L/min/m^2) than subjects in the non-HOHF group (CO, 6.61 L/min ; CI, 2.83 L/min/m^2 ; $p < 0.05$), respectively. The HOHF had significantly greater left ventricular end-diastolic diameter (LVEDD; 5.49 cm) and left ventricular mass index (LVMI; 122.5 g/m^2) compared to the non-HOHF group (LVEDD, 4.73 cm ; LVMI, 80.59 g/m^2).

Differences in leukocyte transcriptomes

A total of 116 DEGs were observed in the HOHF group compared to the non-HOHF group of which 114 were upregulated and 2 were downregulated. The full list of DEGs is provided as supplementary material (**Supplementary Table 1**). **Figure 1** illustrates the clustering of DEGs in a heatmap. An empirical percentile transformation was used, and the rank values of each gene were obtained and then divided by the maximal rank.

IPA of DEGs

The DEGs had significant overlap ($p < 0.05$) with thirty canonical pathways (**Supplementary Table 2**). Of the pathways with significant overlap, only four had a positive z-score when comparing the HOHF group to the non-HOHF group (**Figure 2**). The four canonical pathways that were predicted to be activated in the HOHF group were: 1) sirtuin signaling pathway (z-score=2.000), 2) adenosine monophosphate-activated protein kinase (AMPK) signaling (z-score=1.000), 3) senescence pathway (z-score=0.816), and 4) autophagy (z-score=0.816). Three additional pathways were identified as being activated (Coordinated Lysosomal Expression and Regulation [CLEAR] signaling pathway [z-score=1.000]) or inhibited (pulmonary fibrosis idiopathic signaling pathway [z-score=-1.000] and g-protein coupled receptor signaling [z-score=-1.000]) but were not statistically significant (**Supplementary Table 3**). Although, these pathways could have potential clinical significance and benefit from additional research using a

Obesity-Related HOHF Transcriptomics

Table 1. Characteristics of the study sample

Characteristics		Non-HOHF (n=6)	HOHF (n=6)	p value	All (n=12)
Age (years)	Median (range)	73.50 (58–86)	61 (39–79)	0.180 [†]	67.50 (39–86)
Birth sex				0.117 [‡]	
Male	No. (%)	3 (50.00%)	4 (66.67%)		7 (58.33%)
Female	No. (%)	3 (50.00%)	2 (33.33%)		5 (41.67%)
Race				0.117 [‡]	
Black or African American	No. (%)	1 (16.67%)	1 (16.67%)		2 (16.67%)
White	No. (%)	5 (83.33%)	2 (33.33%)		7 (58.33%)
Other	No. (%)	0 (0.00%)	3 (50.00%)		3 (25.00%)
Ethnicity				0.046 ^{*,‡}	
Hispanic or Latino	No. (%)	0 (0.00%)	3 (50.00%)		3 (25.00%)
Not Hispanic or Latino	No. (%)	6 (100.00%)	3 (50.00%)		9 (75.00%)
Height (cm)	Median (range)	170.15 (157.5–185.4)	171.45 (152.4–186.7)	0.699 [†]	170.15 (152.4–186.7)
Weight (kg)	Median (range)	115.8 (96–166.3)	124.06 (79.38–218.54)	0.818 [†]	115.8 (79.38–218.54)
BMI (kg/m ²)	Median (range)	38.19 (35.15–43.58)	39.97 (30.10–80.18)	0.818 [†]	39.21 (30.10–80.18)
Cardiac output (L/min)	Median (range)	6.61 (2.38–7.06)	9.45 (8.10–13.76)	0.002 ^{*,†}	7.58 (2.38–13.76)
Cardiac index (L/min/m ²)	Median (range)	2.83 (1.73–3.54)	4.65 (2.9–5.4)	0.026 ^{*,†}	3.09 (1.73–5.4)
BNP	Median (range)	204.50 (145–247)	262 (138–424)	0.413 [†]	233 (138–424)
Left ventricular					
Ejection fraction (%)	Median (range)	55 (45–60)	61 (55–65)	0.065 [†]	58.5 (45–65)
End diastolic diameter (cm)	Median (range)	4.73 (4.19–5.3)	5.49 (4.6–6.15)	0.041 ^{*,†}	4.87 (4.19–6.15)
End systolic diameter (cm)	Median (range)	3.04 (2.81–3.70)	3.28 (3.04–4.38)	0.310 [†]	3.17 (2.81–4.38)
End systolic volume index (mL/m ²)	Median (range)	21.5 (15.16–25)	24.5 (19–45)	0.180 [†]	23 (15.16–45)
End diastolic volume index (mL/m ²)	Median (range)	52.49 (33.79–69.00)	68.5 (41–107)	0.132 [†]	57.44 (33.79–107.00)
Mass index (g/m ²)	Median (range)	80.59 (78.00–116.17)	122.5 (81–162)	0.041 ^{*,†}	101 (78–162)

HOHF = high output heart failure; BMI = body mass index; BNP = B-type natriuretic peptide.

*Statistically significant (p<0.05), [†]Mann-Whitney U test; [‡]χ² test.

larger sample size. **Figure 3** displays the sirtuin signaling pathway that had the highest activation. All other canonical pathways had a z-score of zero or there are no current data on the activity pattern available in the literature.

Functions analysis associates biological functions and diseases to the study findings. The top 10 diseases and biological functions are displayed in **Figure 4A**. Toxicity Lists and Toxicity Functions were used to link study data to clinical pathology endpoints to understand the molecules that are known to be involved in a particular type of toxicity. Ten significant Toxicity Functions that overlap with DEGs are displayed in **Figure 4B**. A summary of functions analysis is presented in the **Supplementary Tables 4** and **5**.

Upstream analysis identified molecules that may have caused the expression changes between groups through a direct relationship. The top 5 upstream regulators found in this study are listed in **Table 2 (Supplementary Table 6** for all upstream regulators). The activated top molecule was GATA1 which is known as a transcription factor. **Figure 5** displays all the molecules that GATA1 regulates.

The network analysis function identifies how molecules might work together by connecting focus molecules. Eight networks

were identified in the analysis and are listed in the **Supplementary Table 7**. **Figure 6** displays the molecules with predicted relationships in the highest scoring network with nuclear factor kappa-light-chain-enhancer of activated B cells (NF-κB) complex as the focus molecule. This full network included 25 genes that were upregulated and one gene that was downregulated (**Supplementary Figure 1**).

DISCUSSION

In this study, we assessed the differences in the leukocyte transcriptomes of morbidly obese patients with HOHF and those with non-HOHF using RNA-seq. The abundance of leukocytes provides the opportunity to investigate the various mechanisms involved in obesity-related HOHF. While there were interesting differences in the characteristics of the study sample, the sample size was too small to make inferences about the two groups. Although, the increased CO, CI, LVEDD, and LVMI in the HOHF group were representative of the condition. We found that 116 genes in the HOHF group were significantly different from those in non-HOHF group. There were 114 upregulated DEGs and two downregulated DEGs (p<0.05). The disproportionate number of upregulated genes compared to downregulated genes in the HOHF group was an interesting finding that warrants further in-

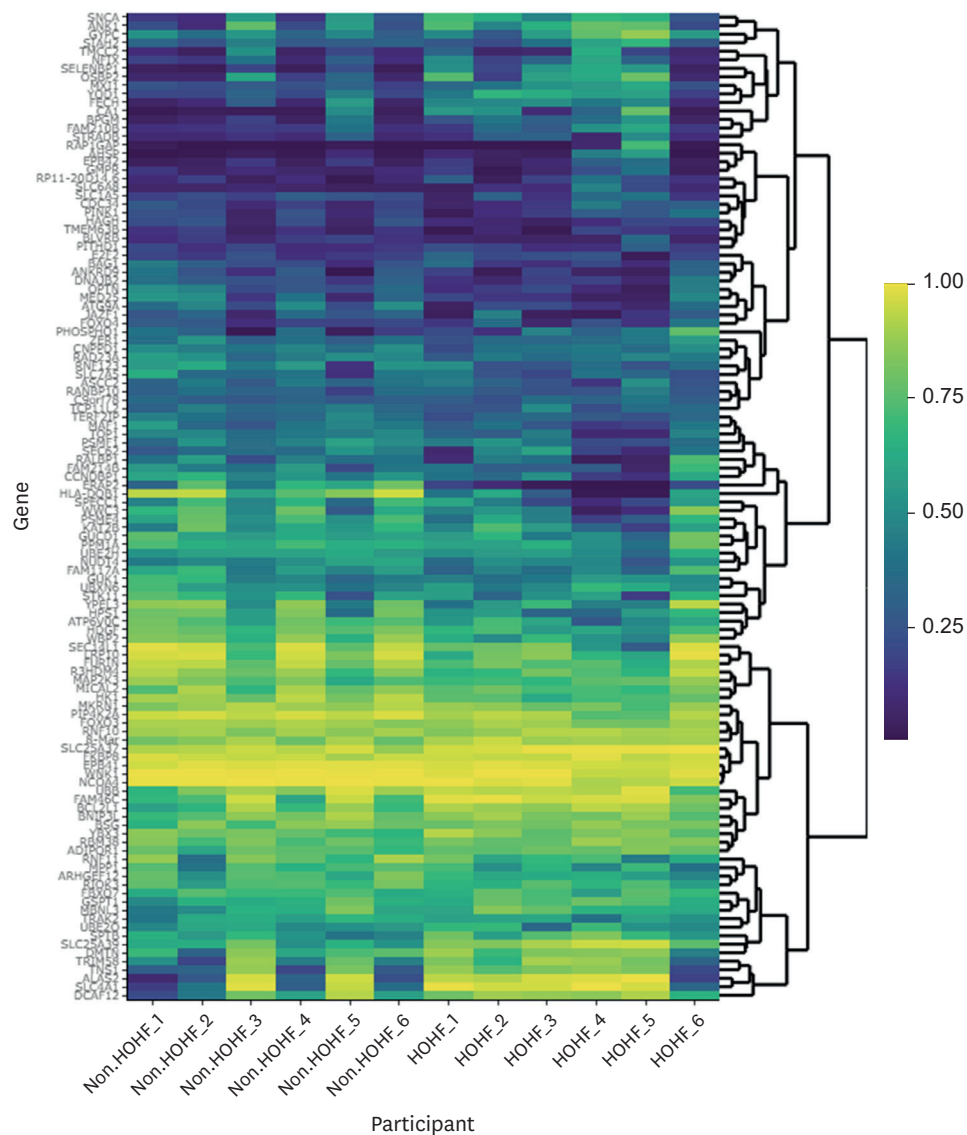


Figure 1. Heat map of differentially expressed genes between the HOHF and non-HOHF groups using empirical percentile transformation. HOHF = high-output heart failure.

investigation in a larger scale study. Possible explanations for the high number of upregulated genes include expression changes due to nutrient depletion from fasting¹¹⁾ or sample processing delays.¹²⁾ Additionally using IPA, we identified the canonical pathways, functional changes, upstream regulator changes, and the mechanistic and causal networks associated with the differential gene expression.

In our analysis, the most significantly upregulated gene was *RAP-IGAP*, a gene that has been found to express in rat cardiomyocyte hypertrophy and mediates angiotensin II-induced cardiomyocyte hypertrophy through its regulation of autophagy and oxidative stress.¹³⁾ This could be a potential therapeutic target for obesi-

ty-related HOHF in humans as treatment with an autophagy agonist and knockdown of the gene by small interfering RNA.¹³⁾ The second most differentiated gene was *CA1*, which is a gene that codes for a protein important in respiratory function, fluid secretion, and maintenance of cellular acid-base homeostasis.

The third most differentiated gene was *ALAS2*, an isoenzyme that catalyzes the precursor for heme synthesis. Overexpression of *ALAS2* is associated with muscle atrophy and mitochondrial dysfunction.¹⁴⁾ Fourth, *AHSP* acts as a scavenger protein and binds to free alpha hemoglobin and prevents aggregation and precipitation that results in the generation of reactive oxygen species. The fifth differentiated gene, *SLC25A39*, has been identified as a

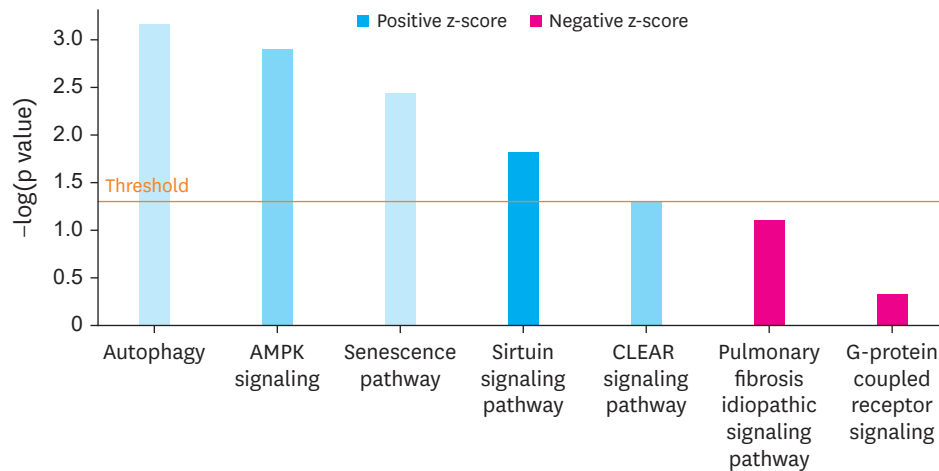


Figure 2. Activated and Inhibited Canonical Pathways associated with differentially expressed genes in peripheral blood leukocytes of the HOHF group compared to the non-HOHF group.

HOHF = high output heart failure; AMPK = adenosine monophosphate-activated protein kinase; CLEAR = Coordinated Lysosomal Expression and Regulation.

mitochondrial glutathione transporter, significant in the heme and iron homeostasis as well as mitochondrial antioxidant response and is rapidly upregulated in response to hypoxia.¹⁵⁾

The canonical pathway analysis predicted the pathways that changed based on DEGs in the HOHF group compared to the non-HOHF group. In this study, the top canonical pathway was the autophagy pathway. The autophagy pathway is important for cardiac structure and function as it removes toxic proteins and damaged organelles.¹⁶⁾ Autophagy is an essential step in the reverse remodeling found during the regression of hypertrophy and increased levels of autophagosomes were positively correlated with better prognosis in patients with dilated cardiomyopathy.¹⁷⁾ Although, multiple studies have posited that overactive or dysregulated autophagy may be associated with decompensated HF.^{18,19)} The increased activation of the autophagy pathway in the HOHF group could either demonstrate the compensatory mechanism that may decline as HF progresses or dysregulated autophagy. Autophagy has been shown to be regulated by the AMPK signaling pathway,²⁰⁾ the second upregulated canonical pathway.

The AMPK signaling helps maintain cellular energy homeostasis by restoring energy balance and adjusting cellular metabolism.²¹⁾ In an animal study that induced HF by pressure overload, it was found that AMPK activation significantly blocked further development of HF and helped restore cardiac function.²⁰⁾ The senescence pathway was the third pathway that was activated in the HOHF group compared to the non-HOHF group. The senescence pathway results in a permanent cell cycle arrest and can lead to increased inflammation.²²⁾ The senescence pathway has been implicated in many inflammatory diseases and age-related pathologies.²³⁾ Santos-Otte and colleagues²³⁾ posited that improvement

in cell signaling by G-protein-coupled receptors could be used as a potential platform to control cellular senescence. Genetic profiles are altered in senescent cells and these cells secrete pro-inflammatory molecules inducing HF.²⁴⁾ Studies testing therapies targeting suppression or elimination of senescent cells could reduce the progression of cardiac disease particularly HF.

In this study, the sirtuin signaling pathway had the highest level of activation. Sirtuins are a class of proteins that have been implicated in energy metabolism, stress response, cell survival, and malignancy.²⁵⁾ There are seven sirtuins distributed in different locations of the cell including the nucleus, cytoplasm, mitochondria, and nucleolus.²⁵⁾ Among the sirtuin family proteins, sirtuin 1 (SIRT1) regulates mitochondrial function by deacetylating nuclear proteins, whereas sirtuin 3 does so by deacetylating mitochondrial proteins.²⁶⁾ **Figure 3** is a partial illustration of the molecules in the sirtuin signaling pathway and their predicted expression in the cytoplasm, nucleus, and mitochondria based on the DEGs from this study. The predicted activation of protein kinase AMP-activated α catalytic subunit (PRKAA; orange inverted triangle in the cytoplasm) triggers numerous pathways that are related to cardiac hypertrophy. PRKAA is responsible for regulating the recycling of damaged mitochondria through autophagy helping to regulate mitochondrial biogenesis, function, and turnover.²⁷⁾ Accumulating evidence suggests that mitochondrial dysfunction plays an important role in the development of cardiac hypertrophy.²⁸⁾ The inhibition of SIRT1 (blue diamond in the nucleus) was worth noting because it led to further activation and inhibition of multiple transcription regulators, enzymes, transporters, and other molecules, contributing to predicted activation of apoptosis and predicted inhibition of oxidative stress. Therefore, it appears that the sirtuin pathway is dysregulated.

Obesity-Related HOHF Transcriptomics

Table 2. Top five upstream regulators of differentially expressed genes in peripheral blood leukocytes of obese patients with HOHF compared to those with non-HOHF

Upstream regulator	Molecule type	Activation z-score	p value of overlap	Target molecules in dataset
KLF1	Transcription regulator		6.58E-14	AHSP, ALAS2, BSG, DMTN, E2F2, EPB41, EPB42, MPP1, SLC4A1, SPTB
GATA1	Transcription regulator	2.849	3.53E-9	AHSP, ALAS2, ANK1, BCL2L1, BLVRB, CA1, DMTN, EPB42, FECH, JAZF1, SLC4A1, SNCA, SPTB
HIPK2	Kinase	2.243	4.86E-9	ALAS2, ANK1, BCL2L1, EPB41, FECH, SLC25A37, SLC4A1, SPTB
EPO	Cytokine	2.199	5.28E-8	ALAS2, ANK1, BCL2L1, BLVRB, BNIP3L, CA1, FECH, GSPT1, KAT2B, SLC4A1, STRADB, TOP1
ABCB6	Transporter	-2.433	7.83E-8	ALAS2, FECH, HAGH, HK1, SLC25A37, SLC25A39

HOHF = high output heart failure; KLF1 = KLF transcription factor 1; AHSP = alpha hemoglobin stabilizing protein; ALAS2 = 5'-aminolevulinate synthase 2; BSG = basigin; DMTN = dematin actin binding protein; E2F2 = E2F transcription factor 2; EPB41 = erythrocyte membrane protein band 4.1; EPB42 = erythrocyte membrane protein band 4.2; MPP1 = MAGUK P55 scaffold protein 1; SLC4A1 = solute carrier family 4 member 1; SPTB = spectrin beta; GATA1 = GATA binding protein 1; ANK1 = ankyrin 1; BCL2L1 = BCL2 like 1; BLVRB = biliverdin reductase B; CA1 = carbonic anhydrase 1; FECH = ferrochelatase; JAZF1 = JAZF zinc finger 1; SNCA = synuclein alpha; HIPK2 = homeodomain interacting protein kinase 2; SLC25A37 = solute carrier family 25 member 37; SLC25A39 = solute carrier family 25 member 39; EPO = erythropoietin; BNIP3L = BCL2 interacting protein 3 like; GSPT1 = G1 to S phase transition 1; KAT2B = lysine acetyltransferase 2B; STRADB = STE20 related adaptor beta; TOP1 = DNA topoisomerase I; ABCB6 = ATP binding cassette subfamily B member 6; HAGH = hydroxyacylglutathione hydrolase; HK1 = hexokinase 1.

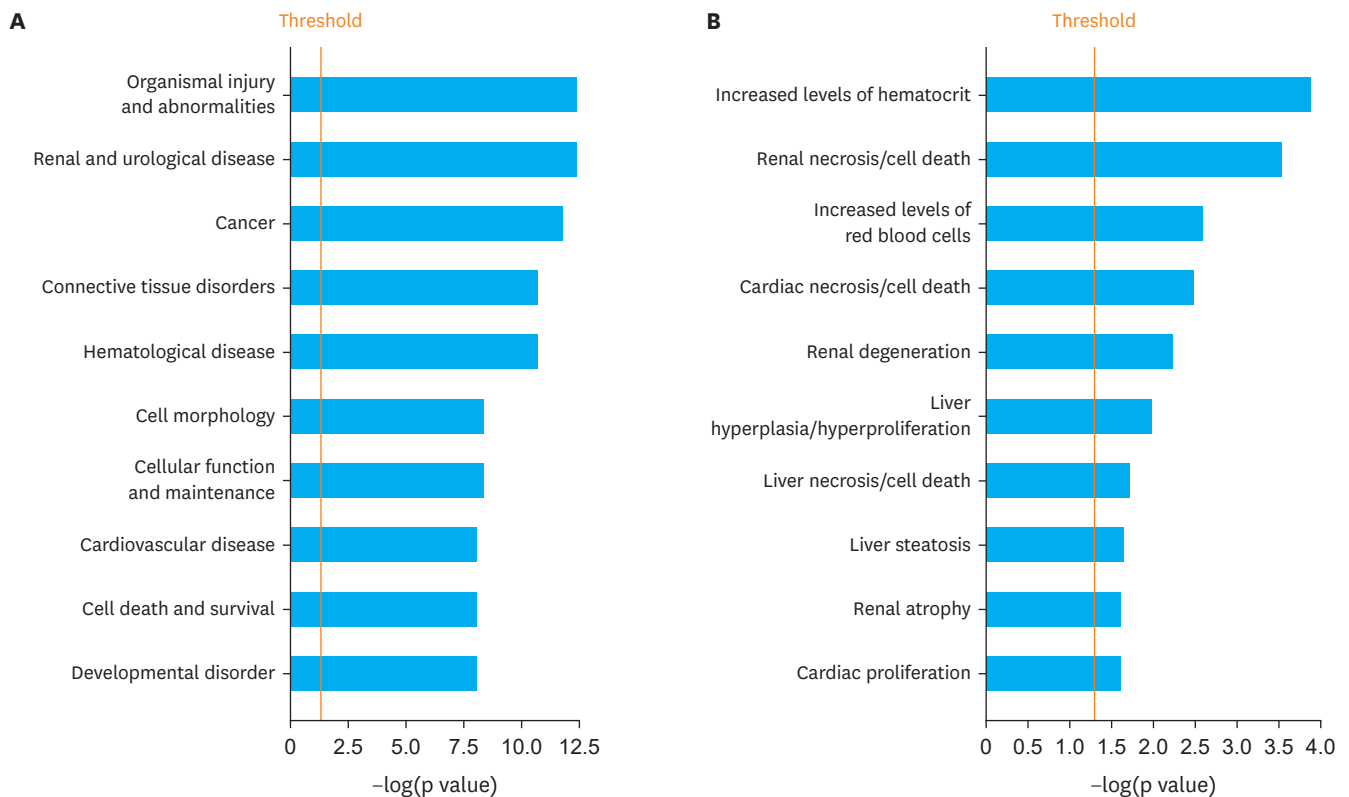


Figure 4. Functions analysis. (A) Top 10 diseases and biological functions. (B) Top 10 toxicity functions.

associating the study findings to diseases such as organismal injury and abnormalities, cellular function and maintenance, cardiovascular disease, and cell death and survival. The toxicity functions were related to levels of hematocrit, cardiac necrosis and proliferation, renal necrosis, and liver necrosis. As these are potential downstream clinical endpoints for the DEGs, they also could be diseases to monitor for obesity-related HOHF. To our knowledge, only Reddy and colleagues²⁾ have characterized pa-

tients with obesity-related HOHF, and the comorbidities were limited to coronary artery disease and hypertension in their single center study. Our findings demonstrate a need to assess for a variety of comorbidities in this patient population to better understand the disease process and presentation.

The upstream regulator analysis was used to predict molecules that may have caused the expression changes between the HOHF

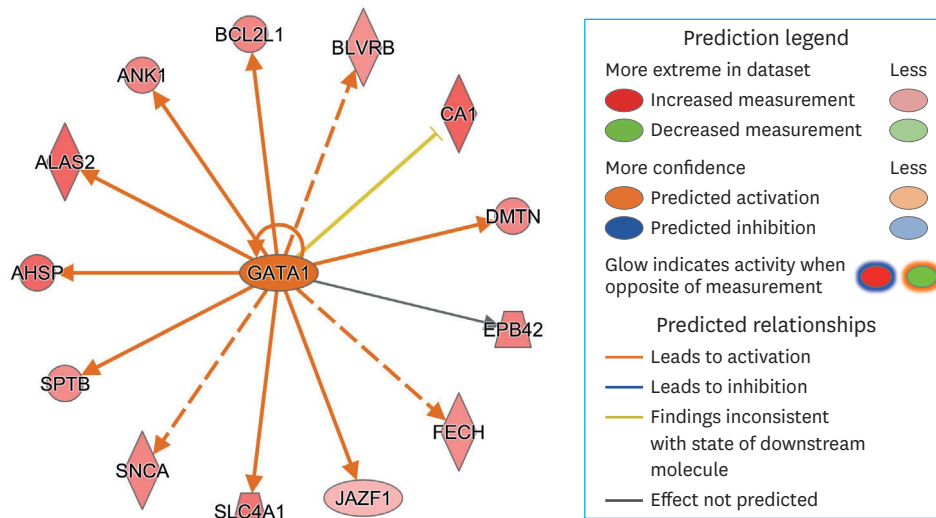


Figure 5. Upstream regulator, GATA1 and relationships with regulated molecules. Solid lines represent a direct interaction. Dashed lines represent indirect interactions. Arrowed lines represent activation, causation, expression, localization, membership, modification, molecular cleavage, phosphorylation, protein-DNA interactions, protein-TNA interaction, regulation of binding, transcription. Lines ended with “⊥” represent inhibition or ubiquitination. Shapes represent molecule type (diamond = enzyme; oval = transcription regulator; trapezoid = transporter; circle = other). GATA1 = GATA binding protein 1; ALAS2 = 5'-aminolevulinatase synthase 2; AHSP = alpha hemoglobin stabilizing protein; ANK1 = ankyrin 1; BCL2L1 = BCL2 like 1; BLVRB = biliverdin reductase B; CA1 = carbonic anhydrase 1; DMTN = dematin actin binding protein; EPB42 = erythrocyte membrane protein band 4.2; FECH = ferrochelatase; GATA1 = GATA binding protein 1; JAZF1 = JAZF zinc finger 1; SLC25A37 = solute carrier family 25 member 37; SLC4A1 = solute carrier family 4 member 1; TOP1 = DNA topoisomerase I.

group and non-HOHF group. The upstream regulator with the greatest overlap in the study dataset was Kruppel-like factor 1 (KLF1), a DNA-binding transcriptional regulator essential for erythropoiesis.³⁰ KLF1 had been identified to play a significant role in cardiomyocyte proliferation in zebrafish and was found to coordinate the networks involved in myocardial differential and mitochondrial metabolisms.³⁰ The second upstream regulator is GATA1, which encodes a protein for a transcription factor important to erythroid development. The next upstream regulator that we identified was homeodomain-interacting protein kinase 2 (HIPK2), a kinase involved in transcription regulation, cellular apoptosis, and regulation of the cell cycle.³¹ HIPK2 has been described as elevated in the myocardium of humans with HF and HIPK2 inhibitors have been shown to prevent cardiomyocyte hypertrophy in a preclinical study but their role in obesity-related HOHF had not been studied.³¹ Another upstream regulator was erythropoietin, a cytokine that is significantly involved in erythropoiesis, but it also has displayed immunomodulatory properties and cardioprotective functions.³² Lastly, the upstream regulator ATP binding cassette subfamily B member 6 (ABCB6) was downregulated when comparing the HOHF group to the non-HOHF group. ABCB6 is a transporter that regulates heme biosynthesis by transporting porphyrins from the cytoplasm to the mitochondria and is also protective against oxidative stress. In this study, the HOHF group expressed genes that are regulated by molecules facilitating red blood cell production and regulation

of the cell cycle, including apoptosis that has been identified to have cardioprotective effects. The difference in these upstream regulators may provide insight to the unique mechanisms underlying obesity-related HOHF.

Ingenuity pathway analysis identifies how molecules work together at the molecular level using network algorithms. The highest scoring network is associated with post-translational modification, cell morphology, and cellular function and maintenance. The activation of NF-κB complexes at the center of this network leads to upregulation of genes encoding for immune responses, apoptosis, proliferation, and differentiation.³³ NF-κB has previously been identified in peripheral leukocytes and cardiomyocytes in individuals with HF.³⁴ NF-κB signaling is a complex that responds to a large variety of immune receptors and is involved in various inflammatory diseases.³³ Thus, our findings support inflammation in cardiac disease and this is the first study to identify genomic markers that differentiate obesity-related HOHF from non-HOHF.

There are several limitations to this study. First, the observational nature of this study limited our data collection to a single time point that does not allow for comparison and understanding of disease progression. The second limitation of the study was the small sample size. The sample recruited for this study was not representative of all obese individuals with HOHF and non-

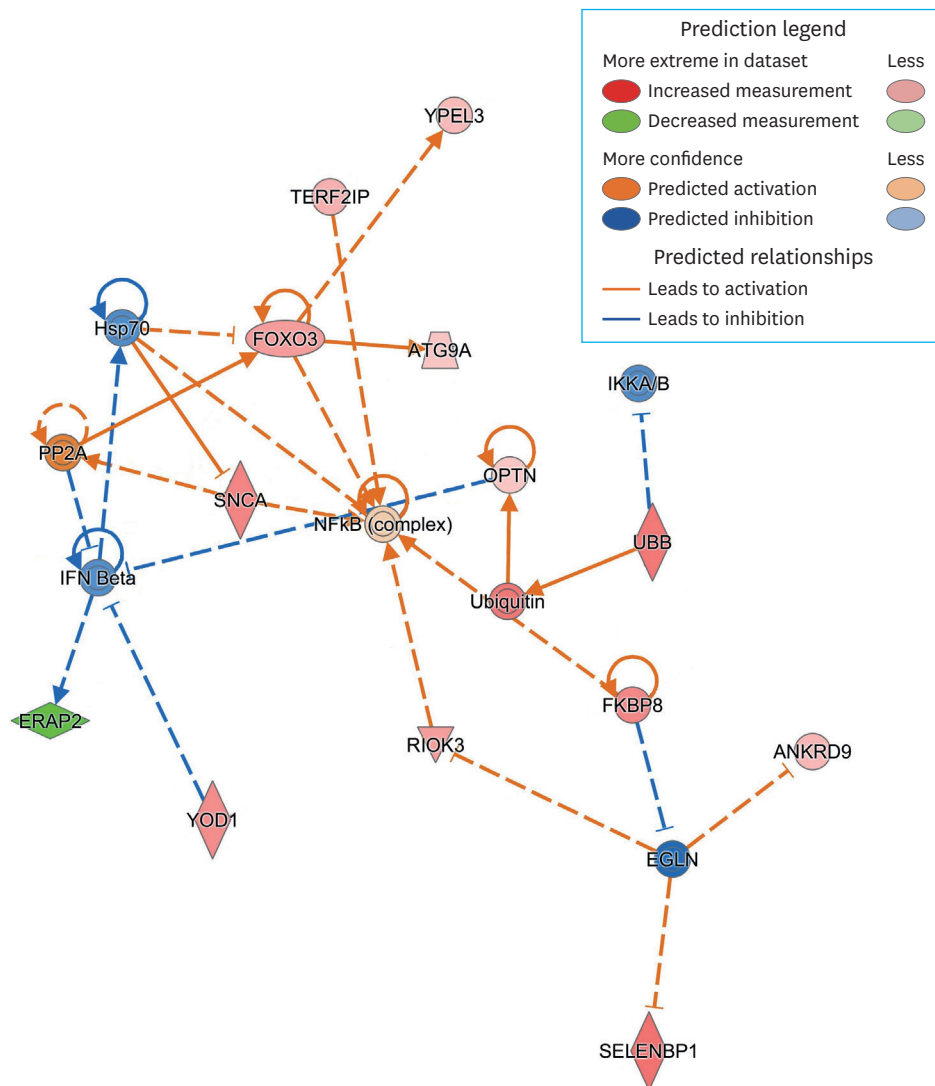


Figure 6. Network 1 post-translational modification, cell morphology, cellular function and maintenance.

ANKRD9 = ankyrin repeat domain 9; ATG9A = autophagy related 9A; EGLN = Egl-9 family hypoxia inducible factor; ERP2 = endoplasmic reticulum aminopeptidase 2; FKBP8 = FKBP prolyl isomerase 8; FOXO3 = forkhead box O3; Hsp70 = heat shock protein 70; IKKA/B = inhibitor of nuclear factor κ B kinase A/B; IFN- β = interferon beta; NF- κ B = nuclear factor kappa-light-chain-enhancer of activated B cells; OPTN = optineurin; PP2A = protein phosphatase 2; RIOK3 = RIO kinase 3; SELENBP1 = selenium binding protein 1; SNCA = synuclein alpha; TERC2IP = TERF2 interacting protein; UBB = ubiquitin B; YPEL3 = Yippee like 3; YOD1 = YOD1 deubiquitinase.

HOHF. Additionally, confounding factors such as social determinants of health should also be further evaluated as contributing to this disease. A third limitation was only utilizing leukocytes to analyze differential gene expression. While leukocytes have been identified as a potential biomarker in HF⁽⁶⁾ with easy access, utilizing and corroborating the genetic markers in multiple types of cells may have been beneficial for analysis and would help identify cell-specific biomarkers. A fourth limitation of this study was only utilizing obese patients with non-HOHF as the comparison group. While this was helpful in identifying the differences between these types of HF, there may be a difference in gene expression in obese patients that do not have heart disease or

non-obese patients with heart disease. A fifth limitation was the infrequent occurrence of patients with obesity-related HOHF receiving planned right heart catheterization. The increased length of time for recruitment resulted in samples being stored in the freezer for over 6 months, possibly resulting in RNA degradation. Due to these limitations, we recommend additional studies be conducted to validate DEGs, evaluate our findings in a more diverse sample, and assess additional confounding factors.

In conclusion, this study identified key differences in gene expression in the leukocyte transcriptomes between the obese individuals with HOHF and non-HOHF. Our findings suggest the

use of leukocytes with RNA-seq provides novel insights into the pathophysiology of obesity-related HOHF. These preliminary findings could be used to discover the underlying mechanisms of obesity-related HOHF and explore new treatments to mitigate progression of disease in the future.

SUPPLEMENTARY MATERIALS

Supplementary Data 1

Supplemental methods

[Click here to view](#)

Supplementary Table 1

DEGs in HOHF group vs. non-HOHF group

[Click here to view](#)

Supplementary Table 2

Statistically significant canonical pathways

[Click here to view](#)

Supplementary Table 3

Non-statistically significant canonical pathways of interest

[Click here to view](#)

Supplementary Table 4

Summary of activated and inhibited biological functions and diseases

[Click here to view](#)

Supplementary Table 5

Summary of activated and inhibited toxicity functions

[Click here to view](#)

Supplementary Table 6

Summary of upstream regulators

[Click here to view](#)

Supplementary Table 7

Summary of networks

[Click here to view](#)

Supplementary Figure 1

Network 1 post-translational modification, cell morphology, cellular function and maintenance.

[Click here to view](#)

Supplementary Figure 2

Sirtuin signaling pathway.

[Click here to view](#)

ORCID iDs

Samantha A. Cintron 
<https://orcid.org/0000-0002-8120-9687>
 Janet Pierce 
<https://orcid.org/0000-0001-7100-7865>
 Mihaela E. Sardu 
<https://orcid.org/0000-0002-3987-7569>
 Diane Mahoney 
<https://orcid.org/0000-0002-9346-0828>
 Jill Peltzer 
<https://orcid.org/0000-0002-8529-5172>
 Bhanu Gupta 
<https://orcid.org/0000-0001-5113-6707>
 Qihua Shen 
<https://orcid.org/0000-0002-1236-0244>

Funding

This study was supported by the Faculty Research Award (PI: Shen), the Office of Grants and Research, School of Nursing, University of Kansas Medical Center, Kansas City, KS, USA; and Crighton Award, School of Nursing, University of Kansas Medical Center, Kansas City, KS, USA.

Conflict of Interest

The authors have no financial conflicts of interest.

Author Contributions

Conceptualization: Cintron SA, Pierce J, Gupta B, Shen Q; Data curation: Sardu ME; Formal analysis: Cintron SA, Sardu ME; Funding acquisition: Shen Q; Methodology: Cintron AS, Pierce J, Gupta B, Shen Q; Resources: Cintron SA, Pierce J, Gupta B, Shen Q; Supervision: Pierce J, Shen Q; Validation: Cintron SA, Pierce J, Mahoney D, Peltzer J, Shen Q; Visualization: Cintron SA, Sardu ME; Writing - original draft: Cintron SA, Pierce J, Shen Q; Writing - review & editing: Cintron SA, Pierce J, Sardu ME, Mahoney D, Peltzer J, Gupta B, Shen Q.

REFERENCES

- Shen Q, Hiebert JB, Rahman FK, Krueger KJ, Gupta B, Pierce JD. Understanding obesity-related high output heart failure and its implications. *Int J Heart Fail* 2021;3:160-71.
[PUBMED](#) | [CROSSREF](#)
- Reddy YN, Melenovsky V, Redfield MM, Nishimura RA, Borlaug BA. High-output heart failure: A 15-year experience. *J Am Coll Cardiol* 2016;68:473-82.
[PUBMED](#) | [CROSSREF](#)

3. Albert CL. Morbid obesity as a therapeutic target for heart failure. *Curr Treat Options Cardiovasc Med* 2019;21:52.
[PUBMED](#) | [CROSSREF](#)
4. Smekal A, Vaclavik J. Adipokines and cardiovascular disease: a comprehensive review. *Biomed Pap Med Fac Univ Palacky Olomouc Czech Repub* 2017;161:31-40.
[PUBMED](#) | [CROSSREF](#)
5. Devaux Y. Transcriptome of blood cells as a reservoir of cardiovascular biomarkers. *Biochim Biophys Acta BBAMol Cell Res* 2017;1864:209-16.
[PUBMED](#) | [CROSSREF](#)
6. Meier S, Henkens M, Heymans S, Robinson EL. Unlocking the value of white blood cells for heart failure diagnosis. *J Cardiovasc Transl Res* 2021;14:53-62.
[PUBMED](#) | [CROSSREF](#)
7. Liew CC, Ma J, Tang HC, Zheng R, Dempsey AA. The peripheral blood transcriptome dynamically reflects system wide biology: a potential diagnostic tool. *J Lab Clin Med* 2006;147:126-32.
[PUBMED](#) | [CROSSREF](#)
8. Robinson MD, McCarthy DJ, Smyth GK. edgeR: a Bioconductor package for differential expression analysis of digital gene expression data. *Bioinformatics* 2010;26:139-40.
[PUBMED](#) | [CROSSREF](#)
9. Galili T, O'Callaghan A, Sidi J, Sievert C. heatmaply: an R package for creating interactive cluster heatmaps for online publishing. *Bioinformatics* 2018;34:1600-2.
[PUBMED](#) | [CROSSREF](#)
10. Qiagen. IPA user manual. Hilden [Internet]. Germany; Qiagen; [cited 2021 May 27]. Available form: <https://qiagen.my.salesforce-sites.com/KnowledgeBase/KnowledgeNavigatorPage?categoryName=IPA>.
11. Peeters JG, Picavet LW, Coenen SG, et al. Transcriptional and epigenetic profiling of nutrient-deprived cells to identify novel regulators of autophagy. *Autophagy* 2019;15:98-112.
[PUBMED](#) | [CROSSREF](#)
12. Meißner T, Seckinger A, Hemminki K, et al. Profound impact of sample processing delay on gene expression of multiple myeloma plasma cells. *BMC Med Genomics* 2015;8:85.
[PUBMED](#) | [CROSSREF](#)
13. Gao Y, Zhao D, Xie WZ, et al. Rap1GAP mediates angiotensin II-induced cardiomyocyte hypertrophy by inhibiting autophagy and increasing oxidative stress. *Oxid Med Cell Longev* 2021;2021:7848027.
[PUBMED](#) | [CROSSREF](#)
14. Peng Y, Li J, Luo D, et al. Muscle atrophy induced by overexpression of ALAS2 is related to muscle mitochondrial dysfunction. *Skelet Muscle* 2021;11:9.
[PUBMED](#) | [CROSSREF](#)
15. Wang Y, Yen FS, Zhu XG, et al. SLC25A39 is necessary for mitochondrial glutathione import in mammalian cells. *Nature* 2021;599:136-40.
[PUBMED](#) | [CROSSREF](#)
16. Woodall BP, Gustafsson AB. Autophagy-A key pathway for cardiac health and longevity. *Acta Physiol (Oxf)* 2018;223:e13074.
[PUBMED](#) | [CROSSREF](#)
17. Saito T, Asai K, Sato S, et al. Autophagic vacuoles in cardiomyocytes of dilated cardiomyopathy with initially decompensated heart failure predict improved prognosis. *Autophagy* 2016;12:579-87.
[PUBMED](#) | [CROSSREF](#)
18. Hein S, Arnon E, Kostin S, et al. Progression from compensated hypertrophy to failure in the pressure-overloaded human heart: structural deterioration and compensatory mechanisms. *Circulation* 2003;107:984-91.
[PUBMED](#) | [CROSSREF](#)
19. Zhu H, Tannous P, Johnstone JL, et al. Cardiac autophagy is a maladaptive response to hemodynamic stress. *J Clin Invest* 2007;117:1782-93.
[PUBMED](#) | [CROSSREF](#)
20. Li Y, Wang Y, Zou M, et al. AMPK blunts chronic heart failure by inhibiting autophagy. *Biosci Rep* 2018;38:BSR20170982.
[PUBMED](#) | [CROSSREF](#)
21. Hardie DG. AMPK as a direct sensor of long-chain fatty acyl-CoA esters. *Nat Metab* 2020;2:799-800.
[PUBMED](#) | [CROSSREF](#)
22. Yan C, Xu Z, Huang W. Cellular senescence affects cardiac regeneration and repair in ischemic heart disease. *Aging Dis* 2021;12:552-69.
[PUBMED](#) | [CROSSREF](#)
23. Santos-Otte P, Leysen H, van Gastel J, Hendrickx JO, Martin B, Maudsley S. G protein-coupled receptor systems and their role in cellular senescence. *Comput Struct Biotechnol J* 2019;17:1265-77.
[PUBMED](#) | [CROSSREF](#)
24. Shimizu I, Minamino T. Cellular senescence in cardiac diseases. *J Cardiol* 2019;74:313-9.
[PUBMED](#) | [CROSSREF](#)
25. Covington JD, Bajpeyi S. The sirtuins: markers of metabolic health. *Mol Nutr Food Res* 2016;60:79-91.
[PUBMED](#) | [CROSSREF](#)
26. Matsushima S, Sadoshima J. The role of sirtuins in cardiac disease. *Am J Physiol Heart Circ Physiol* 2015;309:H1375-89.
[PUBMED](#) | [CROSSREF](#)
27. Koutouroushis C, Sarkar O. Role of autophagy in cardiovascular disease and aging. *Cureus* 2021;13:e20042.
[PUBMED](#) | [CROSSREF](#)
28. Facundo HD, Brainard RE, Caldas FR, Lucas AM. Mitochondria and cardiac hypertrophy. *Adv Exp Med Biol* 2017;982:203-26.
[PUBMED](#) | [CROSSREF](#)
29. D'Onofrio N, Servillo L, Balestrieri ML. SIRT1 and SIRT6 signaling pathways in cardiovascular disease protection. *Antioxid Redox Signal* 2018;28:711-32.
[PUBMED](#) | [CROSSREF](#)
30. Ogawa M, Geng FS, Humphreys DT, et al. Krüppel-like factor 1 is a core cardiomyogenic trigger in zebrafish. *Science* 2021;372:201-5.
[PUBMED](#) | [CROSSREF](#)
31. Zhou Q, Meng D, Li F, et al. Inhibition of HIPK2 protects stress-induced pathological cardiac remodeling. *EBioMedicine* 2022;85:104274.
[PUBMED](#) | [CROSSREF](#)
32. Tanaka T, Nangaku M. Recent advances and clinical application of erythropoietin and erythropoiesis-stimulating agents. *Exp Cell Res* 2012;318:1068-73.
[PUBMED](#) | [CROSSREF](#)
33. Liu T, Zhang L, Joo D, Sun SC. NF- κ B signaling in inflammation. *Signal Transduct Target Ther* 2017;2:17023.
[PUBMED](#) | [CROSSREF](#)
34. Siednienko J, Jankowska EA, Banasiak W, Gorczyca WA, Ponikowski P. Nuclear factor-kappaB activity in peripheral blood mononuclear cells in cachectic and non-cachectic patients with chronic heart failure. *Int J Cardiol* 2007;122:111-6.
[PUBMED](#) | [CROSSREF](#)